



**HAL**  
open science

# Sensitizer-free photon up conversion in (HQ)<sub>2</sub>ZnCl<sub>4</sub> and HQCl crystals: systems involving resonant energy transfer and triplet-triplet annihilation

Amira Samet, Sébastien Pillet, Younes Abid

## ► To cite this version:

Amira Samet, Sébastien Pillet, Younes Abid. Sensitizer-free photon up conversion in (HQ)<sub>2</sub>ZnCl<sub>4</sub> and HQCl crystals: systems involving resonant energy transfer and triplet-triplet annihilation. *Physical Chemistry Chemical Physics*, 2020, 22, pp.1575. 10.1039/c9cp04435c . hal-02903771

**HAL Id: hal-02903771**

**<https://hal.univ-lorraine.fr/hal-02903771>**

Submitted on 7 Dec 2020

**HAL** is a multi-disciplinary open access archive for the deposit and dissemination of scientific research documents, whether they are published or not. The documents may come from teaching and research institutions in France or abroad, or from public or private research centers.

L'archive ouverte pluridisciplinaire **HAL**, est destinée au dépôt et à la diffusion de documents scientifiques de niveau recherche, publiés ou non, émanant des établissements d'enseignement et de recherche français ou étrangers, des laboratoires publics ou privés.



Distributed under a Creative Commons Attribution - NonCommercial 4.0 International License

# Sensitizer-Free Photon Up Conversion in $(\text{HQ})_2\text{ZnCl}_4$ and $\text{HQCl}$ Crystals: Systems Involving Resonant Energy Transfer and Triplet- Triplet Annihilation

Amira Samet<sup>\*a</sup>, Sebastien Pillet<sup>b</sup>, and Younes Abid<sup>\*a</sup>

<sup>a</sup>Laboratoire de Physique Appliquée, Université de Sfax, BP 1171, 3018 Sfax, Tunisia

<sup>b</sup>Universite de Lorraine, BP 239, 54506 Vandœuvre-les-Nancy, France

This work deals with normal luminescence and up-conversion luminescence involving charge transfer and triplet- triplet annihilation in the free lead hybrid materials  $(\text{HQ})_2[\text{ZnCl}_4]$  and  $\text{HQCl}$  salt, HQ is the Hydroxyquinolate cation ( $\text{HQ}^+ = \text{C}_9\text{H}_8\text{NO}^+$ ). The crystal structures were determined by X ray diffraction and the optical properties were investigated by Optical absorption, photoluminescence measurements and electronic band structure calculations. Under UV excitation, the normal luminescence is associated to  $\pi-\pi^*$  transitions within the organic cation and involves energy and charge transfer between inorganic ion and organic cation. Moreover, photoluminescence measurements under various excitation wavelength, performed on the hybrid  $(\text{HQ})_2[\text{ZnCl}_4]$  and the salt  $\text{HQCl}$  have shown an efficient up conversion of light from near infrared (855nm) to visible region at 471nm and 490 nm respectively. This behavior is described as a sensitizer- free up-conversion luminescence based on triplet- triplet annihilation process (TTA-UCL). These compounds are believed to be the first sensitizer-free TTA up-converting materials found in the organic metal halide family. Compared with the conventional TTA-UC solid systems based on precious and heavy metal organic complexes, the title compounds exhibits an efficient photon up-conversion. Furthermore, they have extended the NIR conversion photons to a wide spectral interval of about 300 nm centred around 850 nm

## Introduction.

Processes combining low energy photons to convert them into higher energy photons are known as photon up-conversion (UC). In recent years these processes have proved to be of great interest for various applications, especially to improve the efficiency of photovoltaic cells by extending their spectral operating bands to ranges below the gap (red and near infrared: NIR). Among the mechanisms known hitherto, such as the two-photon absorption (TPA),<sup>1-4</sup> or up conversion based on the energy transfer in lanthanide doped nanocrystals,<sup>5,6</sup> the triplet-triplet annihilation-based up-conversion process (TTA-UC) has attracted great attention as it may occur at lower excitation intensities than other mechanisms,<sup>7-16</sup> such as solar light (a few  $\text{mW cm}^{-2}$  is sufficient, unfocused terrestrial solar irradiance is  $100 \text{ mW cm}^{-2}$ ). In a typical (TTA-UC) mechanism (Figure1), a sensitizer molecule absorbs a low energy photon (long wavelength), creating a singlet excited state that undergoes an intersystem crossing (ISC) to the triplet excited state, this excitation is then transferred to the triplet state of an acceptor molecule or ion that acts as an emitter, then two triplet emitters collide and two excitations fuse into a higher energy singlet excitation which leads to the emission of a photon of higher energy via (TTA) mechanism (Figure1). So far, the best efficiencies were obtained for (TTA-UC)

systems in solutions because of molecular diffusion which favors collisions.<sup>17-19</sup> Moreover, recent studies have been conducted in solid state systems demonstrating that the use of ionic interactions may be a strategy for obtaining competitive efficiencies.<sup>20</sup>

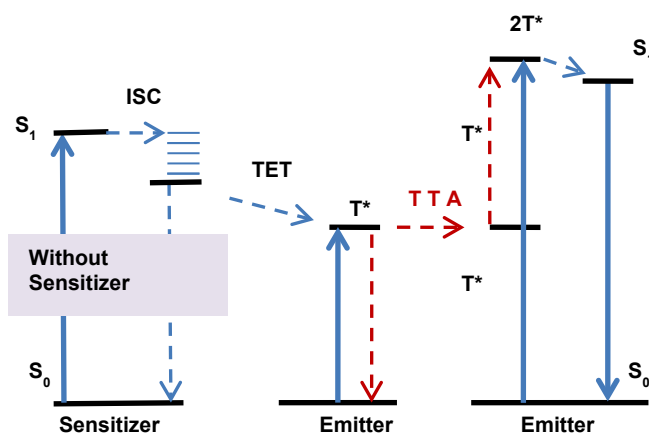


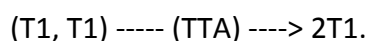
Figure 1: Schematic representations of the triplet – triplet annihilation up-conversion mechanism (TTA- UC, the triplet levels may occur with sensitizer via Inter System Crossing (ISC) or without sensitizer via Spin Orbit Coupling (SOC ) or via Singlet-triplet fission (SF) within the emitter.

Recently, many pioneering works have been reported on new free sensitizer up-conversion systems that do not include heavy or precious metals. In such systems the triplet levels are not populated via ISC mechanism, but rather via spin orbit coupling as for the case of anthracene bromide<sup>21</sup> or via singlet-triplet fission mechanism like that has been described for many organic crystalline systems such as pentacene<sup>22-25</sup> tetracene<sup>22,23</sup> or solid thiophene based organic polymers.<sup>24</sup>

Let's remind that Singlet -Fission mechanism (SF) is described as a bimolecular process occurring between two identical or different organic molecules with aromatic rings. Under IR irradiation the strong interaction between these two chromophores can generate fission of the singlet level into two triplet levels according to the following equation:



Then two triplet levels can again fuse into one level 2T to give the emission of a double energy photon via triplet- triplet annihilation mechanism.



In this work we are mainly interested in a hydroxyl quinilinate Zinc chloride:  $(\text{HQ})_2[\text{ZnCl}_4]$  material, belonging to the vast family of organic metal halides which contains the famous class of inorganic organic perovskite known for their potential interest in the devices. Optoelectronics and Photovoltaics.<sup>26-28</sup> Given the paucity of literature concerning the TTA process in hybrid crystals in general and those based on hydroxyquinoline in particular and in order to investigate the contribution of organic and inorganic entities in this process, we have conducted a comparative study of the hybrid  $(\text{HQ})_2[\text{ZnCl}_4]$  and are HQCl salt. In both compounds, the electronic structure and the stacking of the organic HQ molecules into dimers are typically in favor of an upconversion mechanism involving Singlet fission process followed by triplet annihilation (SF-TTA - UC)

These compounds will be investigated by optical spectroscopy measurements and by theoretical band structure calculations. We will demonstrate below, that these materials may operate as a normal and up conversion luminescent systems involving resonant energy transfer (RET) and (TTA-UCL) mechanism respectively. These compounds would be the first materials of the hybrid organic metalhalides endowed with the property of (TTA-UC) luminescence. These hitherto unrecognized properties turn these compounds and the similar hybrid materials into perspective candidates for potential applications, as up converting materials in photovoltaic conversion, optoelectronic devices or biological imaging.

## II. Materials and methods.

### I.1 Crystal synthesis and structure determination

Single crystals of  $(\text{HQ})_2[\text{ZnCl}_4]$  were synthesized by slow solvent evaporation at room temperature. Firstly, the Hydroxyl quinoline chlorine salt ( $\text{C}_9\text{H}_8\text{NO}\cdot\text{Cl}$ ), abbreviated as (HQ·Cl), was obtained by dissolving ( $\text{C}_9\text{H}_7\text{NO}$ ) in an aqueous HCl (37%) solution. ( $\text{C}_9\text{H}_8\text{NO}\cdot\text{Cl}$ ) salt appears some days later following the remove of residual solvent. Then, 1 mmol of the resulting ( $\text{C}_9\text{H}_7\text{NO}\cdot\text{Cl}$ ) and 1 mmol of  $\text{ZnCl}_2$  were dissolved in HCl solution (37%) and well stirred at ambient temperature. One week later, yellow crystals of  $(\text{HQ})_2[\text{ZnCl}_4]$  were formed.

A good quality single crystals of the hybrid  $(\text{HQ})_2[\text{ZnCl}_4]$  of  $0.30 \times 0.35 \times 0.01 \text{ mm}^3$  were selected for the X ray diffraction. Data collection was carried out, at ambient temperature, on KCCD diffractometer using  $\text{MoK}\alpha$  radiation ( $\lambda = 0.71073 \text{ \AA}$ ). The crystal structure was solved by the direct method and refined by the full matrix least-square technique using the SHELX-97 crystallographic software package.<sup>29</sup> In a separate experiment a single crystal of HQ·Cl salt was selected. The crystal structure was determined at 100K using a Bruker D8 diffractometer equipped with a CMOS PHOTON 100 detector, and using  $\text{MoK}\alpha$  radiation. The unit cell determination and data reduction were performed using APEX2 program suite on the full data set. An empirical absorption correction was applied. The structure was solved by direct methods and successive Fourier difference synthesis, and was refined by full matrix least square method using SHELX-2014 crystallographic software package. All non-H atoms were refined anisotropically. H atoms were located in difference Fourier maps and treated using a riding model, constraining the isotropic displacement parameters to 1.2 Ueq of the parent C atom.

### II.2. Optical measurements.

Optical measurements were performed on thin films of  $(\text{HQ})_2[\text{ZnCl}_4]$  and (HQ·Cl) deposited by spin coating technique on glass substrates. Photoluminescence (PL) as well as Excitation photoluminescence (PLE) measurements were recorded on a Fluoromax-4 Spectrofluorimeter equipped with a xenon lamp as an excitation source. In order to take into account the variation of the excitation intensity over all the UV- visible wavelength range all PL data have been multiplied by a calibration ratio, so that all PL spectra seem to be measured under the same excitation power. Optical absorption (OA) measurements were recorded, on the same samples, using a conventional UV-vis spectrophotometer (HITACHI, U-3300).

### II.3. Electronic band structure calculations.

The calculations were achieved with the modified Becke and Johnson (mBJ)<sup>30</sup> exchange potential in the framework of full-potential linearized augmented plane wave method, as implemented in the Wien2k package.<sup>31</sup> The radius of Muffin-Tin spheres (RMT's) were chosen

in such a way that there was no charge wastage from the core, and therefore total energy convergence was ensured. For a wave function inside the interstitial region, the plane wave cutoff value of  $K_{\text{max}} = 3/\text{RMT}$  was taken. Self-consistency was achieved since the total energy difference between successive iterations was less than  $10^{-5}$  Ryd per formula unit.

### III. Results and discussions

#### 1. Crystal structures

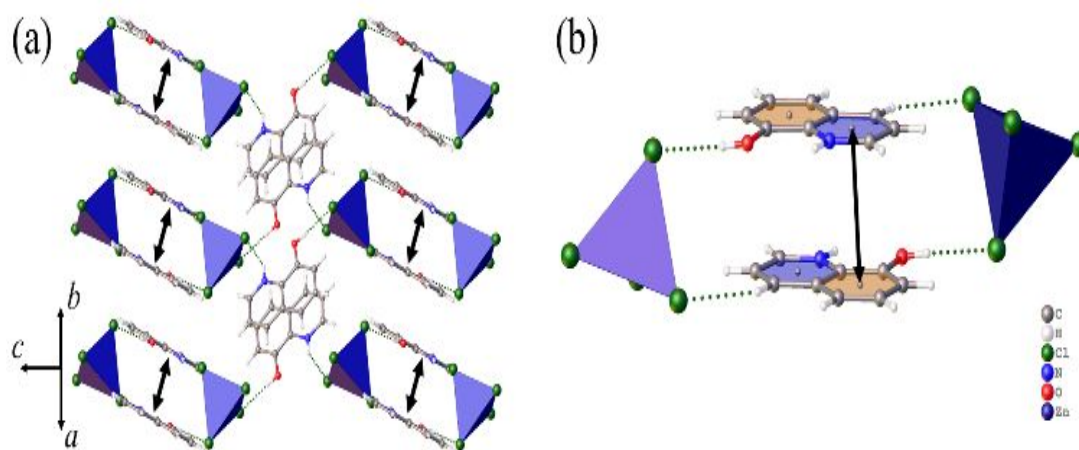


Figure 2. (a) crystal structure packing of  $(\text{HQ})_2[\text{ZnCl}_4]$  projected along  $[110]$  direction and (b) structural arrangement within organic cation. Black arrows depict the intra  $\pi - \pi$  staking interactions, while  $\text{N-H}\cdots\text{Cl}$  and  $\text{O}\cdots\text{Cl}$  hydrogen bonds are shown as dotted lines.

The crystal structure of  $(\text{HQ})_2[\text{ZnCl}_4]$  has been published elsewhere<sup>32</sup>. Briefly,  $(\text{HQ})_2[\text{ZnCl}_4]$  crystallizes in the monoclinic space group  $\text{C2/c}$  with a primitive unit cell of dimensions:  $a = 15.2108(17)$  Å,  $b = 8.1418(8)$  Å,  $c = 16.7204(19)$  Å and four formula units ( $Z = 4$ ). The projection of the crystal structure is shown in Figure 2. It consists of discrete  $[\text{ZnCl}_4]^{2-}$  tetrahedra surrounded by  $(\text{HQ}^+)$  organic cations.  $(\text{HQ}^+)$  cations are associated in interacting dimers through  $\pi - \pi$  staking with centroing distances of  $3.657$  Å and interacting with  $[\text{ZnCl}_4]^{2-}$  ions through  $\text{N-H}\cdots\text{Cl}$  ( $d_{\text{H}\cdots\text{Cl}} = 2.344$  Å) and  $\text{O-H}\cdots\text{Cl}$  ( $d_{\text{H}\cdots\text{Cl}} = 2.284$  Å) hydrogen bonds. The  $\text{HQ}\cdot\text{Cl}$  salt crystallizes in the triclinic  $\text{P-1}$  space group with a primitive unit cell of dimensions:  $a = 7.2651(8)$  Å,  $b = 8.2751(9)$  Å,  $c = 8.4760(9)$  Å,  $\alpha = 78.281(3)^\circ$ ,  $\beta = 86.099(3)^\circ$ ,  $\gamma = 66.537(3)^\circ$ . It consists of  $(\text{HQ}^+)$  organic cations arranged in dimers exhibiting  $\pi - \pi$  stacking interactions with centroid to centroid distances of  $3.554$  Å (Figure 3). The cations are further connected by a network of  $\text{N-H}\cdots\text{Cl}$  ( $d_{\text{H}\cdots\text{Cl}} = 2.36(1)$  Å),  $\text{C-H}\cdots\text{Cl}$  ( $d_{\text{H}\cdots\text{Cl}} = 2.74(1)$  Å) and  $\text{O-H}\cdots\text{OH}_2$  ( $d_{\text{H}\cdots\text{O}} = 1.70(3)$  Å) hydrogen bonds with  $\text{Cl}^-$  counter-ions and lattice water molecules.  $= 2.284$  Å. By comparing the two crystal structures, it is interesting to note that in both cases, the organic cations  $[\text{C}_9\text{H}_8\text{NO}]^+$  are arranged in dimers in both cases, nevertheless, the intermolecular interaction in both crystals show two remarkable differences: (i) in the hybrid material each quinoline molecule is linked to two tetrahedra  $\text{ZnCl}_4$  via ionic bonds  $\text{CH}\cdots\text{Cl}$  and  $\text{OH}\cdots\text{Cl}$ , whereas in the salt each molecule is bound to a chlorine ion via  $\text{CH}\cdots\text{Cl}$  hydrogen bond on one hand and via a Vander walls  $\text{CH}\cdots\text{O}$  bond with neutral water molecule on the other hand, this indicates that the charge transfer is more favored in the hybrid than in the salt.

(ii) The aromatic cycles are closer in the salt than in the hybrid

This specific structural topology induces strong overlap between the molecular orbitals of the cations, and may be related to the observed optoelectronic properties, such as the bleu shift of the PL signal of the hybrid and its enhancement with respect to that of the salt (see below).

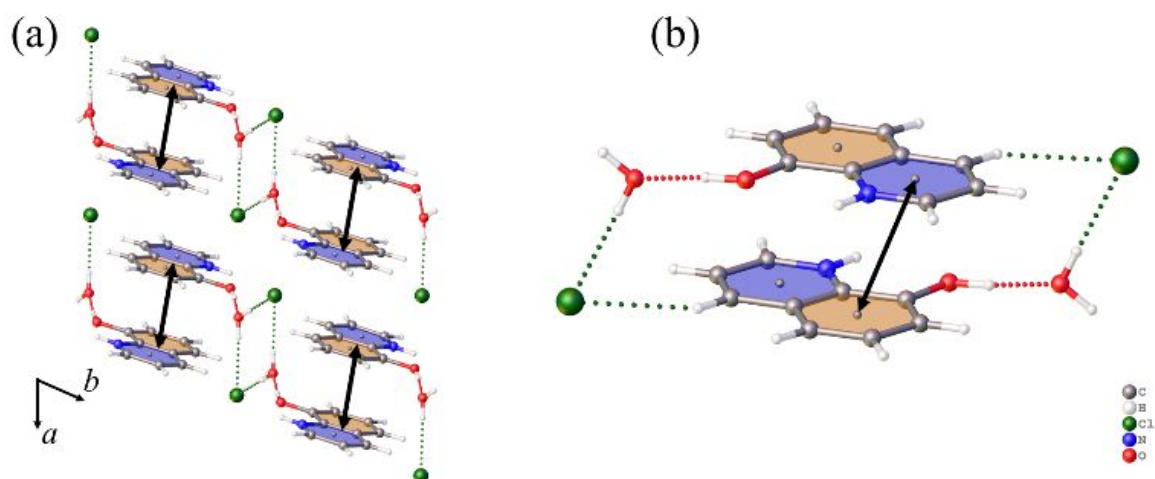


Figure 3. (a) Crystal packing of the HQ.Cl salt projected along the [001] direction, and (b) structural arrangement within organic cation dimers. Black arrows depict the intra-dimer  $\pi$ - $\pi$  stacking interactions, while N-H...Cl, C-H...Cl and O-H...OH<sub>2</sub> hydrogen bonds are shown as dotted lines.

## 2. Density of states and band structure calculations

As for the case of all the hybrid materials containing several molecules per unit cell and involving interactions of different natures (covalent, ionic, Vander walls...), the detailed and rigorous interpretation of the absorption and emission spectra is not so obvious.

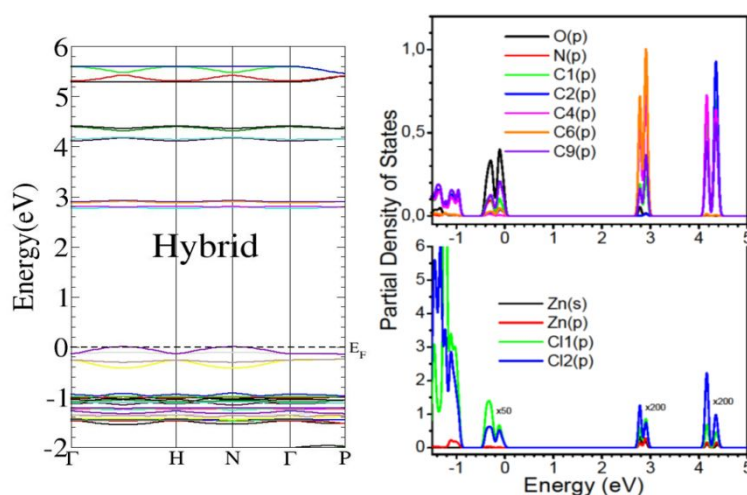


Figure 4. Calculated electronic band structures and electronic density of states of the hybrid (HQ)<sub>2</sub>[ZnCl<sub>4</sub>]

It has been found that in addition to comparisons with peer systems, the calculation of band structures and electronic density of states (DOS) provides an effective tool for accurate and rigorous optoelectronic interpretation. In this context we performed a simulation of (DOS) in

terms of periodic DFT calculation (Figure 4). Let us recall that for conventional IV or III-V semiconductors whose cohesion is ensured by strong covalent bonds, the valence bands and the conduction bands are generally characterized by a large dispersion and by relatively continuous density of states. For our hybrid material, as for the case of homologous materials,<sup>33,34</sup> since it is a crystal formed by organic and inorganic molecular entities interacting with weak bonds of the Van der Waals or hydrogen type, the dispersion curves are fairly flat, and the band structure is formed of several discrete sub bands. It is then more appropriate to use the HOMO-LUMO frontier orbitals notions for each type of molecule, rather than valence band and conduction band.

In Figure 4 is illustrated the calculated electronic band structure along the high symmetry points of the Brillouin zone of  $(\text{HQ})_2[\text{ZnCl}_4]$  hybrid compound. Partial densities of states of the  $(\text{HQ})_2[\text{ZnCl}_4]$  hybrid compound are also plotted in Figure 4. The same calculations were made for the  $(\text{HQ}.\text{Cl}.\text{H}_2\text{O})$  salt (see supplementary informations). As we can see in the same figure, the optical band gap is estimated at 2.63 eV (471 nm). It is also obvious that the valence band maximum is composed namely of O(2p) and C(2p) organic atomic orbitals, with a little contribution of Cl1(3p) and Cl2 (3p) inorganic ones. Whereas, the lowest levels of the conduction band, rather the sub band sweeping the energy range from 2.65 eV to 3eV, correspond closely to the orbitals of carbon C(2p) and nitrogen N (2p) atoms of the organic molecule with a slight contribution of Zn(s,p) and Cl (p) orbitals. These results may indicate that in this material the conjugated electrons are strongly involved in electronic transitions and charge transfer, contrary to similar compounds based on non-conjugated organic ligands in which the inorganic part mainly contributes to the valence band. Moreover, the alignment of energy levels of the quinoline  $\pi$ -conjugated cation with those of the inorganic  $[\text{ZnCl}_4]^{2-}$  anion may be at the origin of an enhancement of carrier mobility in the hybrid structure. We will see below, that the results obtained by the semi-local mBJ method are in perfect agreement with those of the experimental data. Indeed, the mBJ exchange potential allows the calculation of band gaps with a precision similar to that with the very expensive Green function calculations,<sup>35</sup> and therefore has the capability to overcome the well-known shortcoming of the DFT-based methods in predicting the band gaps.

### 3. Optical properties.

#### 3.1 Normal photoluminescence

As we have mentioned, because of the existence of two luminescent entities in the same crystal, the organic cation ( $\text{HQ}^+$ ) on the one hand and the inorganic  $[\text{ZnCl}_4]^{2-}$  ion on the other hand, and in order to distinguish and analyze the contribution of each ion in the process of emission, we have systematically performed optical absorption (OA), photoluminescence (PL), and photoluminescence excitation (PLE) measurements on the  $(\text{HQ}.\text{Cl})$  salt as well as on the  $(\text{HQ})_2[\text{ZnCl}_4]$  crystals. As seen in Figure 5, The optical absorption spectra of both  $(\text{HQ})_2[\text{ZnCl}_4]$  compound and  $(\text{HQ}.\text{Cl})$  salt show the same shape consisting of two wide absorption bands with maxima around 315nm (3.93 eV) and 370nm (3.35 eV) associated to deep levels of the organic cation.

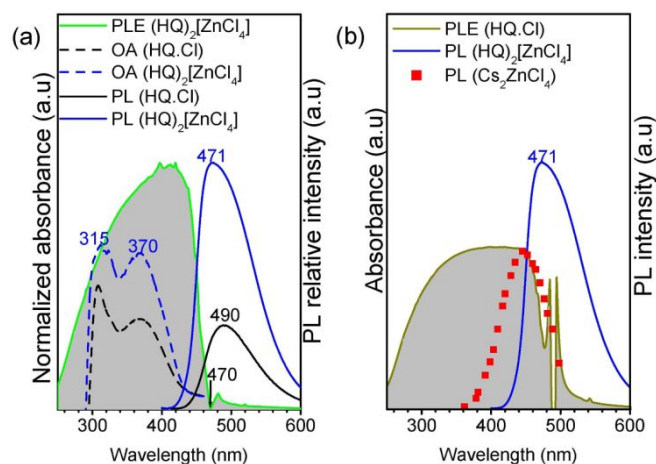


Figure 5: Optical Absorption, PL and PLE spectra of  $(\text{HQ})_2[\text{ZnCl}_4]$  and the salt  $\text{HQCl}$ . For comparison the PL spectra of  $\text{Cs}_2\text{ZnCl}_4$  is drawn according to the reference (36). PL measurements were performed under 375 nm excitation.

Whereas, the PLE measurements show a very broad excitation band, covering entirely the optical absorption bands and leading to an optical gap of 2.63 eV (471 nm). Many recent works were carried out on hybrid compounds based on  $\text{ZnCl}_4$  and containing optically inactive molecules such as  $(\text{DMA})_2\text{ZnCl}_4$ ,<sup>36</sup>  $(\text{APC})_2\text{ZnCl}_4$ <sup>37</sup> and  $[\text{C}_7\text{H}_{16}\text{N}_2][\text{ZnCl}_4]$ <sup>38</sup>, these works reveal that  $\text{ZnCl}_4$  ions are characterized by a broad absorption band between 300 nm and 400 nm corresponding to an HOMO-LUMO gap around 3.1 eV, whereas the photoluminescence was measured only for  $\text{Cs}_2\text{ZnCl}_4$  and shows a PL band around 450 nm (2.75 eV).<sup>39</sup> The obtained results are in well agreement with the calculated band structure, confirming the alignment of the electronic levels associated with the  $(\text{HQ}^+)$  organic cation and the  $[\text{ZnCl}_4]^{2-}$  anion as predicted by the DFT simulation. Moreover, as seen in Figure 5, the photoluminescence spectrum recorded under 375 nm excitation is characterized by an extremely intense line at 471 nm fairly coinciding with the PLE band limit, compared with the PL spectrum of the  $(\text{HQCl})$  salt, this line originates from the  $\pi$ - $\pi^*$  transitions within the organic molecule. The blue shift from 490 nm in the salt to 471 nm in the crystal is due to the stacking of the aromatic rings of  $(\text{HQ}^+)$  cation and their interaction with  $[\text{ZnCl}_4]^{2-}$  anion.

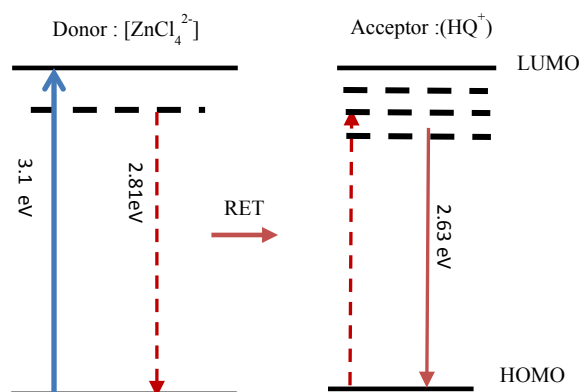


Figure 6: Energy diagram of the electronic structure of the  $(\text{HQ})_2[\text{ZnCl}_4]$  crystal. The relevant energy levels include the HOMO, LUMO levels for  $[\text{ZnCl}_4]^{2-}$  anion and  $(\text{HQ}^+)$  cation. The red dashed lines correspond to the nonradiative transitions outlining the conversion of inorganic excitation to an organic excitation.



The results we have at this stage lead to an energy diagram for the  $(\text{HQ})_2[\text{ZnCl}_4]$  crystal described by a wide HOMO-LUMO of 3.1 eV associated with the inorganic anion  $[\text{ZnCl}_4]^{2-}$  with an inorganic excitonic level at 2.81 eV which is resonant with electronic levels of the organic  $(\text{HQ}^+)$  cation. This diagram (Figure 6) suggests an interaction between the inorganic and the organic ions involving resonance energy transfer (RET).<sup>40,41</sup> One must recall that RET is a dipole interaction which describes at the molecular scale the transfer of energy (or charges) between two chromophores (molecules or ions): a donor (D) entity having a high HOMO-LUMO band Gap and an acceptor entity (A) with a smaller HOMO-LUMO band Gap. This interaction is conditioned by mainly two criteria: (i) the distance between the acceptor and donor entities must not exceed few nanometers, and (ii) the donor emission spectrum must overlap significantly the absorption spectrum of the acceptor. In the case of  $(\text{HQ})_2[\text{ZnCl}_4]$  both criteria are quite satisfied. In fact as seen above in figure 5(b), the emission band of  $[\text{ZnCl}_4]^{2-}$  (Donor) has a significant overlap with the excitation spectra of the (HQ) cation (Acceptor). In addition, from the X ray diffraction measurement, it is noticeable that  $\text{ZnCl}_4$  tetrahedra are linked with (HQ) organic cations through  $\text{N-H}\cdots\text{Cl}$  and  $\text{O-H}\cdots\text{Cl}$  bonds of 2.344 Å and 2.285 Å lengths respectively, which is in favor of the Dexter charge transfer.<sup>42</sup> Furthermore, as described above, the DFT density-of-state calculation demonstrates a coincidence of the electronic levels of the hybrid ZnCl bond with those of organic cation, a fact which is in favor of the energy and charge transfer between the anionic  $[\text{ZnCl}_4]^{2-}$  tetrahedra and the  $(\text{HQ}^+)$  cation. Thereby, the intense luminescence of the title compound results from radiative recombinations occurring within the  $\text{HQ}^+$  organic cation. As illustrated in Figure 6, under the 375 nm incident laser,  $\text{ZnCl}_4$  inorganic excited carriers will be transferred to the  $\pi^*$  levels of the organic cation via Dexter charge transfer process, leading to the enhancement of organic photoluminescence. The blue shift of the organic emission from 2.5 eV in the salt to 2.63 eV in the hybrid stems from the intermolecular interactions between aromatic rings of organic cations (Figure 2 and 3). Furthermore, as seen in figure 5a, we notice an enhancement by up to 3 orders of magnitude the emission intensity in  $(\text{HQ})_2[\text{ZnCl}_4]$  compared to that of the salt  $\text{HQCl}$ . This can be explained by the fact that in the hybrid compound the crystalline cohesion is ensured by ionic interactions which are in favour of energy and charge transfer, whereas in the salt are added the Vander walls interactions with neutral water molecules that are less favourable for these transfer mechanisms.

### 3.2 Up conversion photoluminescence

So far, to the best of our knowledge, no up-conversion studies have been performed on ZnCl-based hybrid crystals or on crystals containing the hydroxyl quinoline entity. In the present work, in order to characterize the resonant energy transfer, we carried out a systematic study of photoluminescence under variable excitation ranging from UV to IR (250nm to 900nm), surprisingly, we found in addition to the normal luminescence described above, a photoluminescence under IR excitation. In figure 7 we represent the variation of the photoluminescence band at 471 nm as a function of the excitation wavelength.

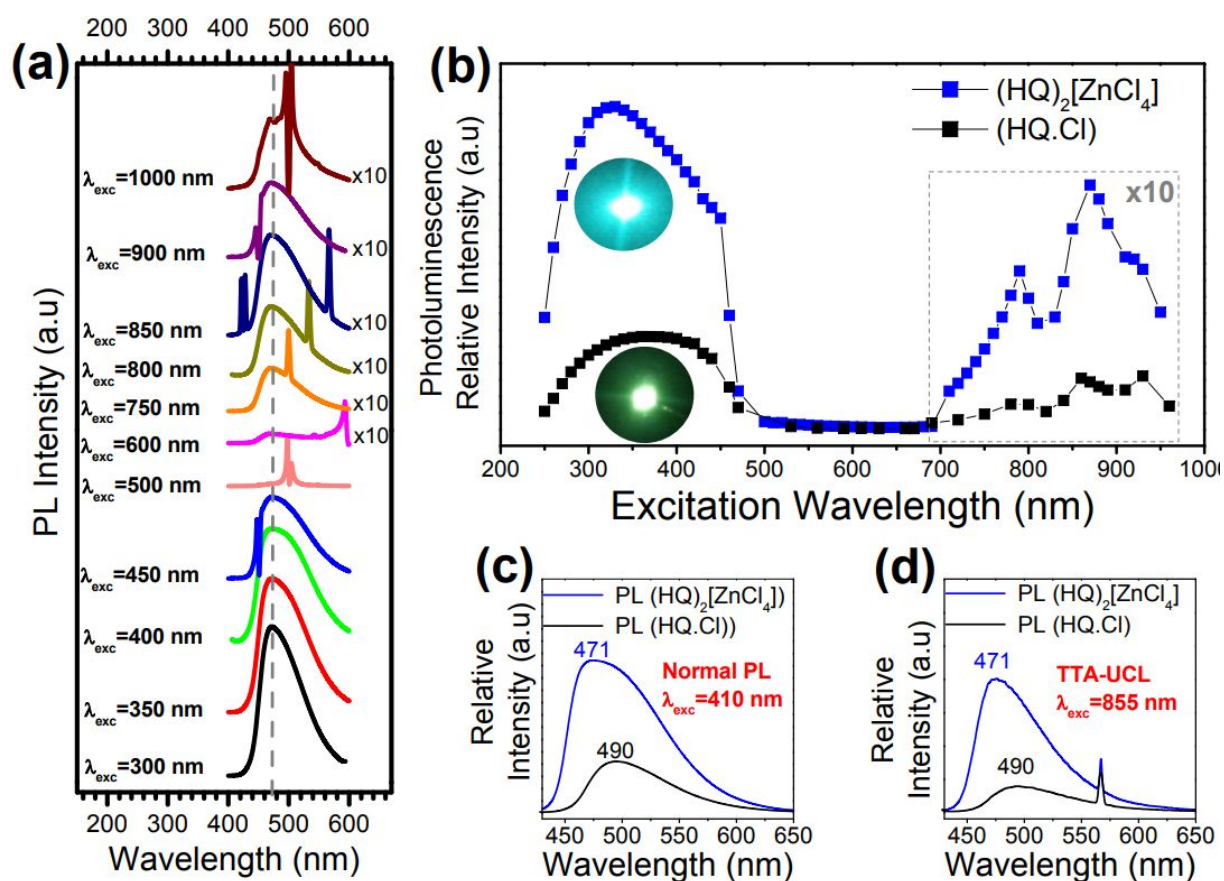


Figure 7: (a) PL spectra of  $(\text{HQ})_2[\text{ZnCl}_4]$  under different excitation wavelengths. (b) Intensity of PL spectra of the  $(\text{HQ})_2[\text{ZnCl}_4]$  compound and the  $(\text{HQ.Cl})$  salt as function of excitation wavelengths, (c) Comparison of PL spectra of  $(\text{HQ})_2[\text{ZnCl}_4]$  and  $(\text{HQ.Cl})$  under 400 nm (Normal PL) and (d) Comparison of PL spectra of  $(\text{HQ})_2[\text{ZnCl}_4]$  and  $(\text{HQ.Cl})$  under 855 nm (up-conversion luminescence). In (a) and (b) all data were multiplied by a calibration ratio to take into account the variation of the excitation power with the excitation wave length.

As we can see, for the UV-Blue excitation, an intense luminescence is observed for wavelengths between 250 nm and 500 nm and the intensity reaches the maximum around 350 nm, then the intensity drops off steeply for excitation between 500 and 700 nm. For wavelengths between 700 and 1000 nm the photoluminescence signal reappears and reaches its maximum under the excitation around 855 nm. For a reliable investigation of the up-conversion mechanism and in order to determine the role of each of the organic and inorganic components, we have carried out, in the same conditions, photoluminescence measurements under different excitations on the hybrid material as well as on the organic cation in the salt. The results are illustrated in figure 7. We note that for both hybrid and salt materials, for the same infrared excitation range around 850 nm we obtain the same emission spectrum in the visible region around 470 nm and 490 nm respectively. In addition, the PL spectra show the same profile and differ only in intensity. This result indicates that in both normal and up-conversion regimes, the emission processes involve radiative recombination occurring between the same initial and final electronic states. These comparative measurements lead to the following deductions:

(i) in both up and normal regimes the emission originates mainly from the organic cation.

(ii) the TTA – UC process occurs without sensitizer, a fact which is expected as the  $\text{Cl}^-$  and  $[\text{ZnCl}_4]^{2-}$  ions are not endowed with singlet or triplet levels that can absorb in the IR and NIR regions.

Among the possible free - sensitizer mechanisms, it seems that the singlet - fission process followed by triplet-triplet annihilation perfectly describes this up-conversion process from NIR to visible region. As we have already pointed out, many recent studies have been carried out on up-conversion systems involving singlet fission (SF) processes such as pentacene<sup>22-25</sup> tetracene<sup>22,23</sup> or solid thiophene based organic polymers.<sup>24</sup>

In these studies it has been established that SF is conditioned mainly by the following criteria: (i) SF is a bimolecular process occurring between two chromophore molecules containing at least two aromatic rings and the energy of the singlet level is almost equal to twice the energy of the triplet level

(ii) in the solid state, the  $\pi$  stacking of aromatic rings and their interaction favours and facilitates SF process

(iii) the triplet exciton diffuses from a molecule to an other via Dexter transfer which consists of an electron exchange at short distances not exceeding 1 nm.

For both materials studied herein, all these criteria are perfectly satisfied indeed:

(i) The quinoline ( $\text{HQ}^+$ ) cation has two aromatic rings and has singlet energy levels (1.45 eV , 413nm) greater than double the triplet energy level (2,91 eV , 426 nm).

(ii) The structural study by XRD showed that the  $\text{HQ}^+$  cations are associated in pairs and their interaction favours the SF process.

(iii) The XRD measurements have also shown that the interaction distances  $\pi$ - $\pi$  between two cation is of the order of 3.5 and 3.6 Å which allows the overlap of wave functions between neighbouring molecules to facilitate the Dexter transfer.

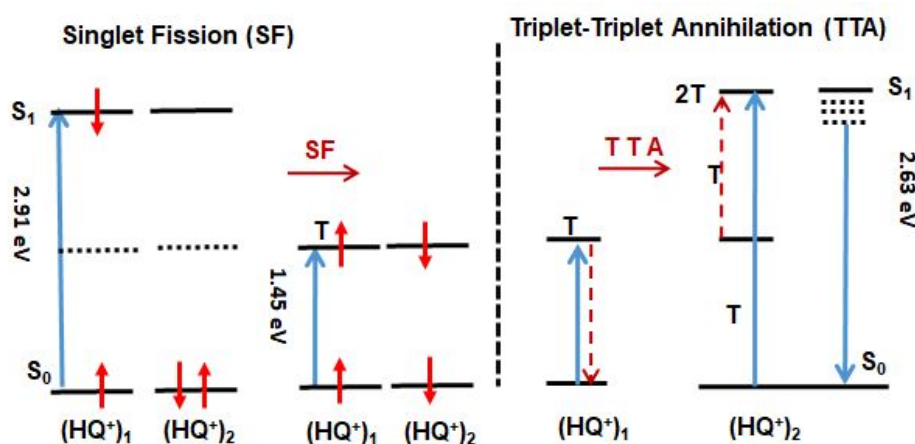


Figure 8: Schematic representations of the sensitizer free TTA- UC mechanism: The fission of two singlet states into two triplet states occurring into two interacting  $\text{HQ}^+$  cation is followed by an emission via triplet – triplet annihilation (TTA) .

Consequently, as we have described in the figure 8, the TTA-UC process may be tentatively explained as follows, under infrared excitation, the strong interaction between organic  $\text{HQ}^+$  cations favour the fission of singlet excitonic level into two triplet levels , once the triplet levels of two neighbouring  $\text{HQ}^+$  cation are populated, an energy transfer occurs in a such manner that two triplet levels are fused into a double energy excitation (2T) and which then gives rise to an emission of a photon of higher energy via TTA.<sup>43,44</sup> Furthermore, as seen in

figure 7, we observe an enhancement by up to 5 orders of magnitude of the up converted emission intensity in the hybrid material compared to that of the salt. This can be explained by the fact that in the hybrid compound the crystalline cohesion is ensured by ionic interactions which are in favour of energy migration and charge transfer, whereas in the salt are added the Vander walls interactions with neutral water molecules that are less favourable for these transfer mechanisms. Accordingly, as we mentioned above, in this work we report the first result that describes a sensitizer- free process. We notice that, compared to the conventional two-component solid state TTA-UC systems, sensitizer-free TTA-UC ones are pertinent to compensate for energy losses, following the intersystem crossing of the sensitizers and the triplet energy migration (TEM) from sensitizer to emitter. It is also worthy to note that organic up conversion systems based on TTA-UC have been extensively used for improvement of solar cells efficiencies. The best up converting material has reached a wavelength limit of 790 nm,<sup>45</sup> with an up conversion efficiencies up to 28%.<sup>46</sup> Nevertheless, it has proved challenging to find long-lived organic chromophores that allow up-conversion systems to operate beyond 800 nm. The up-converter material reported here is believed to be of great potential interest, as it could extend the NIR conversion photons at wavelengths as long as 855 nm. This near IR spectral domain is of particular interest because the conventional absorber semiconductors in solar cells, like silicon ( $E_g = 1.1$  eV) and CdTe ( $E_g = 1.5$  eV) as well as the absorber perovskites ( $E_g = 1.6$  eV)<sup>47</sup> are unable to collect low energy photons whose wavelengths exceed 1200 , 800 and 765 nm respectively. Moreover, previous studies, relating to TTA converters, show that infrared spectral intervals converted to visible do not exceed few tens of nanometers.<sup>48,49</sup> Whereas for the studied compound, the width of the converted interval is remarkably larger and reaches 300nm, allowing to harness a greater fraction of the solar spectrum, a fact which further increases the interest of these materials for improving the efficiency of photovoltaic cells.

### Conclusion.

In this work, we have studied the optical properties of the inorganic organic hybrid crystals  $(HQ)_2[ZnCl_4]$  in which, the two components  $HQ^+$  and  $[ZnCl_4]^{2-}$  are two chromophores having quite close HOMO-LUMO gaps. The study of the luminescence as function of the exciton showed an intense emission signal around  $470\text{ nm}^{-1}$  that it can be observed under UV excitation or under excitation in the near infrared (up conversion). The comparative study showed that the normal photoluminescence involves a resonant energy transfer mechanism in which  $ZnCl_4^{2-}$  acts as donors and  $HQ^+$  acts as an acceptor, whereas the up-conversion luminescence is governed by the sensitizer-free triplet- triplet annihilation (TTA). In addition,  $(HQ)_2[ZnCl_4]$  is the first TTA up-converting material discovered in the family of organic metal halide crystals, which is promising for the improvement of solar cells efficiency as it has extended the conversion of infrared light to a wider spectral range. Given the band gap tunability depending on the nature of the organic molecule, this opens a new path way for improving solar cell performance. Moreover, considering that Zinc is the least harmful metal for the human body, such up-conversion material can be good candidate for biological imaging applications. Therefore, we believe that by the discovery of the first TTA up converter material in the hybrid perovskite family and their derivatives, this work will enrich this class of materials by arousing a renewed research on low cost, eco-friendly raw materials, with facile synthesis and excellent optical properties at room temperature.

## Conflicts of interest

The authors declare no conflict of interest.

**Keywords:** Hybrid materials. Photo upconversion · Triplet-triplet annihilation · organic metal halides

## Acknowledgements

This work was partly supported by :

(i) ERANETMED project :132- Energy “HYDROSOL”

(ii) Ministry of high education of Tunisia.

(II) CNRS, French PIA project “Lorraine Université d'Excellence”, reference ANR-15-IDEX-04-LUE.

## References

1. Pawlicki, M. ; Collins, H. A. ; Denning, R. G. ; Anderson, H. L.,. *Chem. Int. Ed.* **2009**, *48*, 3244.
2. Göppert-Mayer, M., *Ann. Phys.* **2009**, *18*, 466.
3. Ye, C.; Zhou, L.; Wang, X.; Liang, Z., *Phys. Chem. Chem. Phys* **2016**, *18*, 10818.
4. Terenziani, F.; Katan, C.; Badaeva, E.; Tretiak, S.; Blanchard-Desce, M. *Adv. Mater* **2008**, *20*, 4641.
5. Gibart, P.; Auzel, F.; Guillaume, J.-C.; Zahraman, K. . *Jpn. J. Appl. Phys.* **1996**, *35*, 4401.
6. Auzel, F. *Chem. Rev.* **2004**, *104*, 139.
7. Singh-Rachford, T. N. ; Castellano, F. N.. *Coordination Chemistry Reviews* **2010**, *254*, 2560.
8. Monguzzi, A.; Tubino, R.; Hoseinkhani, S.; Campione, M.; Meinardi, F. *Phys. Chem. Chem. Phys.* **2012**, *14*, 4322.
9. Kim, J.-H.; Kim, J.-H. *J. Am. Chem. Soc.* **2012**, *134*, 17478.
10. Simon, Y. C.; Weder, C. J. *Mater. Chem.* **2012**, *22*, 20817.
11. Gray, V.; Dreos, A.; Erhart, P.; Albinsson, B.; Moth-Poulsen, K.; Abrahamsson, M. *Phys. Chem. Chem. Phys.* **2017**, *19*, 10931.
12. Schulze, T. F.; Schmidt, T. W. *Energy Environ. Sci.* **2015**, *8*,103..
13. Häring, M.; Pérez-Ruiz, R.; Jacobi von Wangelin, A.; Díaz, D. D. *Chem. Commun.* **2015**, *51*, 16848.
14. Yanai, N.; Kimizuka, N. *Acc. Chem. Res.* **2017**, *50*, 2487.
15. Huang, Z.; Tang, M. L. *J. Am. Chem. Soc.* **2017**, *139*, 9412.
16. Hill, S. P.; Hanson, K. J. *Am. Chem. Soc.* **2017**, *139*, 10988.
17. Singh-Rachford, T. N. ; Castellano, F. N. *Coordination Chemistry Reviews* **2010**, *254*, 2560.
18. Balushev, S.; Miteva, T.; Yakutkin, V.; Nelles, G.; Yasuda, A.; Wegner, G. *Phys. Rev. Lett.* **2006**, *97*, 143903.
19. Zhao, J.; Ji, S.; Guo, H. *RSC Advances* **2011**, *1*, 937.
20. Ogawa, T.; Yanai, N.; Fujiwara, S.; Nguyen, T.-Q.; Kimizuka, N. *J. Mater. Chem. C*, **2018**, *6*, 5609.
21. Okumura, K.; Matsuki, M.; Yamada, T.; Yanai, N.; Kimizuka, N.. *ChemistrySelect* **2017**, *2*, 7597.
22. Xianfeng Qiao, Dongge Ma, *Materials Science&EngineeringR* (2019) in press doi.org/10.1016/j.mser.2019.100519
23. Sanders et al., *Chem* (2019), impress, doi.org/ 10.1016/j.chempr.2019.05.012
24. Natalie A. Pace, et al, *The Journal of Physical Chemistry Letters* **2017**, *8*, 24, 6086-6091 .
25. Andrew B et al, *Adv. Mater.* **2017**, *29*, 1701416.
26. Wang, Y. et al. *Nano Lett.* **2016**, *16*, 448.
27. Xu, Y. et al. *J. Am. Chem. Soc.* **2016**, *138*, 3761.
28. Chen, W.; Bhaumik, S.; Veldhuis, S. A.; Xing, G.; Xu, Q.; Grätzel, M. ; ... Sum, T. C. *Nat. Commun.* **2017**, *8*, 15198.
29. Sheldrick, G. M. *SHELXL-97*, Program for Crystal Structure Refinement; University of Göttingen: Germany, 1997.
30. Tran, F.; Blaha, P. *Phys.Rev. Lett.* **2009**, *102*, 226401.
31. Blaha, P.; Schwarz, K.; Madsen, G. K. H.; Kvasnicka, D.; Luitz, J. *WIEN2K*, An Augmented Plane Wave and Local Orbitals Program for Calculating Crystal Properties; Schwarz, K., Ed.; Vienna University of Technology: Austria, **2001**.
32. Khakhlyar, P.; Baruah, J. B. *J. Chem. Sci.* **2015**, *127*, 215.
33. Samet, A.; Triki, S.; Abid, Y. *J. Phys. Chem. C* **2019**, *123*, 6213.
34. Barkaoui, H.; Abid, H.; Yangui, A.; Triki, S.; Boukheddaden, K.; Abid, Y. *J. Phys. Chem. C* **2018**, *122*, 24253.
35. Tran, F.; Blaha, P. *Phys. Rev. Lett.* **2009**, *102*, 226401.

36. N.Mahfoudha et al., *Physica B: Condensed Matter* **2019**, 554, 1126-136
37. DineshJasrotiaa Sanjay et al, *Materials Chemistry and Physics* **2018**, 207, 98-104
38. Ben Hadj Sadoket al. (2018). *Journal of Physics and Chemistry of Solids*. In press, doi:10.1016/j.jpccs.2018.12.039
39. Sugawara, K.; Koshimizu, M.; Yanagida, T.; Fujimoto, Y.; Haruki, R.; Nishikido, F.; ... Asai, K. *Opt Mater* **2015**, 41, 53.
40. D'Innocenzo, V. et al, *Nat Commun* **2014**, 5,4586.
41. Stryer, L. *Annu. Rev. Biochem.* **1978**, 47, 819.
42. Dexter, D. L. *Chem. Phys.* **1953**, 21, 836.
43. Monguzzi, A.; Tubino, R.; Meinardi, F. *Phys. Rev. B.* **2008**, 77, 155122.
44. McClure, D. S. *J. Chem. Phys.* **1949**; 17, 665.
45. Yakutkin, V et al, *Chem. Eur. J.* **2008**, 14, 9846.
46. Zhou, J.; Liu, Q.; Feng, W.; Sun, Y.; Li, F. *Chem. Rev.* **2015**, 115, 395.
47. Bush, K. A et al. *Nat. Energy* **2017**, 2, 17009.
48. Briggs, J. A.; Atre, A. C.; Dionne, J. A. *J. Appl. Phys.* **2013**, 113, 124509.
49. Zhao, J.; Ji, S.; Guo, H. *RSC Adv.* **2011**, 1, 937.